RESEARCH ARTICLE
doi: 10.2306/scienceasia1513-1874.2024.073

ScienceAsia 50 (4): 2024: ID 2024073: **1–9**

Inhibitory activity of mangiferin against *Porphyromonas gingivalis* gingipain K, a causal agent of Alzheimer's disease: An integrated *in vitro* and *in silico* study

Sheri-Ann Tan[a,*], Jia Hui Lai[b], Su Ying Lee[a], Xin Yan Loh[a], Shi Ruo Tong[c], Wei Quan Ong[b], Muhamad Zakwan Hafiq bin Abdul Razak[b], Yien Yien Ong[a], Siew Lee Cheong[b,*]

[a] Department of Bioscience, Faculty of Applied Sciences, Tunku Abdul Rahman University of Management and Technology, Setapak, Kuala Lumpur 53300 Malaysia

[b] Department of Pharmaceutical Chemistry, School of Pharmacy, International Medical University, Bukit Jalil, Kuala Lumpur 57000 Malaysia

[c] Department of Physical Science, Faculty of Applied Sciences, Tunku Abdul Rahman University of Management and Technology, Setapak, Kuala Lumpur 53300 Malaysia

[*]Corresponding authors, e-mail: tansw@tarc.edu.my, CheongSiewLee@imu.edu.my

Received 12 Jun 2023, Accepted 8 May 2024
Available online 20 Aug 2024

ABSTRACT: Gingipain K, a virulence protein from *Porphyromonas gingivalis*, is involved in the pathogenesis of Alzheimer's disease. Hence, this research aimed to investigate the potential of methanolic extract of *Cratoxylum cochinchinese* leaves (CME) and the pure compound, mangiferin, in inhibiting this protein. The inhibition of gingipain K activity was measured based on the cleaving potential of this enzyme towards Ac-Lys-pNA, a synthetic peptide substrate containing a chromogenic leaving group. Phytocompounds present in CME were then used as ligands in a simulated docking study with gingipain K. Results indicated that the CME was a potential inhibitor of gingipain K, reducing the protein activity in a dose dependent manner compared with the untreated control. Molecular docking analysis of the phytocompounds revealed mangiferin as the best inhibitor with the highest docking score. The studies showed that mangiferin engaged in H-bonding and π-π interactions with important active site residues in vicinity, such as Asp388, Gly445, Cys477, Trp391, and Trp513. The compound, when tested in the *in vitro* gingipain K inhibition assay, produced an IC_{50} of 134.20 μM, which was close to the IC_{50} of the positive control, TLCK (IC_{50} = 108.40 μM). The additional bioactivity of mangiferin as gingipain K inhibitor as reported here together with its known neuroprotective activity shall encourage further investigation of this molecule in the treatment of such a debilitating illness, the Alzheimer's disease.

KEYWORDS: *Porphyromonas gingivalis*, gingipain K, *Cratoxylum cochinchinense*, mangiferin, Alzheimer's disease

INTRODUCTION

Porphyromonas gingivalis is an asacharolytic, non-motile, anaerobic Gram-negative bacterium that has been identified as a keystone pathogen for periodontitis [1]. Recently, this bacterium is detected in the cerebrospinal fluid (CSF) of subject diagnosed with Alzheimer's disease (AD) [2]. Intriguingly, one of its virulence proteins, gingipain K (Kgp), a trypsin-like cysteine protease enzyme, is found in abundance in the cerebral cortex of AD brain, and the enzyme is found to play a critical role in the pathogenesis of this disease [3].

The neurotoxicity of this protease was reported both *in vitro* and *in vivo*. The enzyme was able to break down Tau protein through proteolysis [3]. It was previously shown capable to activate caspase-3 leading to both Tau phosphorylation [4] and cleavage [5]. Deterioration of Tau by Kgp resulted in hyperphosphorylation of this protein, which led to formation of insoluble paired helical filaments (PHFs) that eventually grew into neurofibrillary tangles (NFTs) [6]. *P. gingivalis* synthesised outer membrane vesicles (OMVs) enriched with Kgp were rapidly internalised into mammalian cells, activating NLRP3 inflammasome and initiating the formation of ASC speck which caused cell death through pyroptosis [7]. Activation of NLRP3 inflammasome in microglia and liberation of ASC specks triggered β-amyloid (Aβ) aggregation and deposition [8]. It was also revealed that intraneuronal Kgp stimulated neuronal NLRP1, leading to neuronal cell death and secretion of neuroinflammatory interleukins IL-1β and IL-18 [3]. In addition, triggering receptor expressed on myeloid cells 1 (TREM1) was previously shown to be degraded by Kgp as well [3]. The degeneration of TREM1 by Kgp resulted in dysregulation of Aβ phagocytosis in the central nervous system and induced chronic inflammation which further damaged the brain cells [9]. Apolipoprotein E4 (APOE4) was also reported as another target of Kgp. It was cleaved by this enzyme through proteolysis and produced neurotoxic fragments that caused the formation of Aβ plaque and disruption of normal functioning of neurons in AD brain [10]. As such, Kgp is regarded as an important target in the pathogenesis of AD that warrants further investigation.

In the past, a number of naturally derived and synthetic molecules were reported to inhibit the Kgp

of *P. gingivalis*. Natural inhibitors were characterised through the screening of bioactive substances while synthetic inhibitors were designed and synthesised based on the specificity of the active site. The natural inhibitors of Kgp were mostly derived from plants such as canavanine in sword bean extract (SBE) [11], catechins in green tea extract [12], Sanggenol A from *Morus alba* root bark [13], and quercetin [14]. Likewise, Kgp activities could also be suppressed by synthetic inhibitors such as KYT-36 [15], COR119, COR271 [3], A71561, and tetracyclines [16]. However, these molecules proved unsuitable in *in vivo* studies due to their interference with important host proteolytic enzymes [16]. Hence, inhibitors from natural sources, especially from plants are much promising in this regard.

Cratoxylum cochinchinense is a perennial tree species widely distributed in Southeast Asia. It is classified under the *Hypericaceae* family and is known as 'tue gliang' in Thailand. This plant has been broadly used as traditional medicine to treat numerous illnesses such as itches, cough, diarrhea, burns, fever, and abdominal pain [17]. Previous findings reported that different parts of *C. cochinchinense* plant (leaves, stems, barks, branches and twigs, fruits, resins, and roots) contained abundance of polyphenolic compounds such as xanthones [18], tocotrienols, anthraquinones [19], and triterpenoids [20]. The leaves specifically were found to contain phenolic components such as mangiferin, vismiaquinone A, α-tocopherol, δ-tocotrienol, and canophyllol, a triterpene [1].

The polyphenolic mangiferin had demonstrated noteworthy efficacy in neurodegenerative diseases, including Alzheimer's disease (AD) and Parkinson's disease [21]. A 60-day oral dose of mangiferin restored the morphology of neurons and mitochondria in the hippocampus region of accelerated aging and dementia mice models, resulting in close-to-normal, more compact, and ordered structure. Treatment with this compound was also found to reduce the aggregation of β-amyloid (Aβ) [22]. Furthermore, a 6-week continuous intragastric administration of mangiferin exhibited beneficial effects on formaldehyde-induced neurotoxicity (AD-like model) in both *in vitro* and *in vivo* studies. This effect was attributed to the inhibition of crosstalk between endoplasmic reticulum stress and the hyperphosphorylation of Tau protein, involving downstream kinases like GSK-3β and CaMKII [23]. The highlighted morphological and biochemical improvements were corroborated by enhanced learning and memory performance in AD mice models tested using Morris water maze, Y-maze, and Novel Object Recognition (NOR) examinations [22, 23]. Collectively, these findings underscore the potential of mangiferin as a promising therapeutic agent in the context of Alzheimer's disease.

Importantly, *C. cochinchinense* leaves extract was recently shown to inhibit citrullination activity of peptidyl arginine deiminase (PAD), another virulence protein from *P. gingivalis*, linked to AD. Its phytocompound, mangiferin displayed potential inhibitory effect *in silico* towards this bacterial PAD as well [1]. Therefore, in this study, we investigated the Kgp inhibitory activities of the methanolic leave extract of *C. cochinchinense* and the pure compound, mangiferin, through *in silico* and *in vitro* approaches. Both CME and mangiferin, if potent, could be a novel treatment for Alzheimer's disease.

MATERIALS AND METHODS

Plant extraction

C. cochinchinense was obtained from a local farm, Herbal Oasis, located in Negeri Sembilan, Malaysia. The plant was identified, and the voucher specimen (Voucher No: MFI 0229/21) was deposited at Herbarium, Biodiversity Unit, Universiti Putra Malaysia. The leaves of *C. cochinchinense* were cleaned and dried in the oven at 40 °C until a constant weight was obtained. The dried leaves were ground into fine powder and stored in an airtight bag under 4 °C. The extraction was done by macerating 200 g of dried leaves in a 1:10 (w/v) ratio of 80% methanol. After 48 h, approximately 200 ml of the 80% methanol was collected and 500 ml of fresh 80% methanol was then added. This process was repeated every two days and the extract solvent was collected on the ninth day of maceration. The extract solvent was filtered and concentrated by a rotary evaporator to obtain the methanolic extract of *C. cochinchinense* (CME). The CME was stored in a −20 °C freezer [1] until use.

Cultivation of *P. gingivalis*

40.0 g of Trypticase Soy Agar (TSA), 5 g of yeast extract and 5 ml of 1 mg/ml hemin were added into 1000 ml of distilled water in a flask and autoclaved. 10 ml of filter sterilised and freshly prepared 5% L-cysteine and 2 ml of 0.5 mg/ml menadione (Vitamin K; Sigma-Aldrich, Germany) were pipetted into the flask before preparation of agar plates. The TSA plates were then pre-reduced for a minimum of 24 h by placing them in an anaerobic condition at 37 °C. The *P. gingivalis* strain (ATCC 33277) was inoculated on the media by using four quadrant streak plate method. The TSA-plates were then incubated anaerobically at 37 °C for 7 days for bacterial growth [24].

Gingipain K enzymatic assay

Assay was performed based on published works with minor modifications [24]. *P. gingivalis* bacteria from a seven-day culture on agar plates were suspended in gingipain assay buffer, containing 200 mM Tris-hydrochloride (Tris.Cl) pH 7.6, 5 mM calcium chloride ($CaCl_2$), 150 mM sodium chloride (NaCl), and

0.02% sodium azide (NaN_3) with freshly neutralised 10 mM L-cysteine HCl, to an OD_{660} of 0.03. Then, 100 µl of this mixture was added into the wells of the 96-well flat-bottom plate prior to the addition of 90 µl of test samples of different concentrations. For the negative and positive controls, 90 µl of samples were replaced with 1% dimethyl sulfoxide (DMSO) and 50 µM N-α-tosyl-L-lysine-chloromethylketone hydrochloride (TLCK; Sigma-Aldrich), respectively. Then, 0.5 mM substrate, N-α-acetyl-L-lysine-4-nitroanilide hydrochloride (Ac-Lys-ρNA; Bachem, Fisher Scientific, USA), was added to each well, except for the blank control. The absorbance of the solutions was read at the wavelength of 405 nm using a Tecan Infinite M200 PRO microplate reader (Tecan, Switzerland) over a period of 15 min. The protease activity was then obtained by subtracting the background absorbance (negative control) from the individual samples. The IC_{50} graphs of percentage of Kgp inhibition against concentrations were plotted using GraphPad Prism version 9.

Molecular docking of selected ligands against Kgp

Molecular docking simulation of five main phytochemicals (Fig. 1), namely mangiferin (**1**), vismiaquinone A (**2**), δ-tocotrienol (**3**), α-tocopherol (**4**), and canophyllol (**5**) [1, 18–20] present in the leave extract of *C. cochinchinense* was performed on the *P. gingivalis* Kgp (PDB ID: 6I9A) [15] *via* Schrödinger modeling software (Maestro version 12.7) [25]. The structure of each ligand was prepared and optimised via LigPrep [26] before the docking. The structure was minimised under OPLS-2005 force field; the possible ionization states of the structure at neutral pH 7 were generated by using Epik program. Tautomers and stereoisomers of the structure were also generated; for each ligand, at most 8 tautomers and 32 stereoisomers per ligand were set to be generated. The crystal structure of the Kgp was downloaded from the Protein Data Bank and prepared using the Protein Preparation module [27] in Maestro. Missing hydrogens were added, and bond orders were assigned. Crystallographic waters were removed, and hydrogen bonding networks were automatically optimised by using PROPKA set at pH 7. The heavy atoms were minimised under OPLS-2005 force field with converging the heavy atoms to RMSD = 0.3 Å. Docking grid was centered on the binding site of the co-crystallised ligand, KYT-36 with grid coordinates of x: 3.41, y: −12.18, z: 11.12. The grid box encompassed the active site residues consisting of Asp388, His444, Gly445, Cys477, Trp391, Tyr512, Trp513 and His575 [15]. The docking calculations were carried out using Glide Standard Precision (SP) protocol [28]. During docking, active site residues were kept rigid while flexible ligand sampling was used. Post-docking minimization in the field of receptor was performed to produce better poses of ligand. Binding poses and interactions of each compound with adjacent residues of the binding pocket were subsequently analysed. Binding pose with the highest docking score was selected for each compound. Docking score is the sum of GlideScore and state penalty for a given protonation or tautomeric state for a ligand, known as Epik state penalty; GlideScore is an empirical scoring function to rank-order ligands and separate ligands with strong binding affinity from those with little to no binding ability [28].

Quantification of mangiferin through high performance liquid chromatography (HPLC)

Mangiferin was identified through HPLC (Thermo Scientific Dionex Ultimate 3000, USA) coupled with Eclipse Plus C18 column (Agilent, USA; 4.6 × 250 mm; 5 µm) using the Agilent 1260 DAD spectrum of 254 nm. The mobile phase of HPLC consisted of (A) 1.5% (v/v) of phosphoric acid in water and (B) acetonitrile. It was performed on an isocratic solvent system of 25% of B at a flow rate of 0.8 ml/min. The column temperature was maintained at 40 °C. The absolute quantity of mangiferin in *C. cochinchinense* was determined based on comparison with the standard curve (Fig. S1) of mangiferin pure compound (ChemFaces, China). The injection volume of the standard and sample (1 mg/ml) for analysis was 1 µl. All standards and samples for injection were filtered through 0.2 µm nylon membrane prior to the analysis.

Statistical analysis

Statistical analyses of results obtained from the Kgp enzymatic assay of plant extract were performed as follows: the data were first tested for homogeneity of variances by the test of Levene; for multiple comparisons, one-way ANOVA was followed by Bonferroni test when variances were homogeneous, or by Tamhane test when variances were not homogeneous. SPSS program (version 19.0) was used. Unpaired t-test was employed to compare the IC_{50} of mangiferin and TLCK inhibitory actions. IC_{50} was generated using GraphPad Prism (version 9). All data were tested at the level of significance where $p < 0.05$.

RESULTS

Kgp enzymatic assay for CME

P. gingivalis cell lysate was used to investigate the inhibitory properties of CME against the activities of Kgp. TLCK was selected as the positive control for the inhibition of Kgp. A dose dependent increase in the inhibitory activities of the plant extracts towards Kgp was observed from concentrations of 0.0625 to 0.25 mg/ml. The inhibitory action of CME at 0.25 mg/ml (29.41%) was found to be as effective as the positive control (33.45%) (Fig. 2).

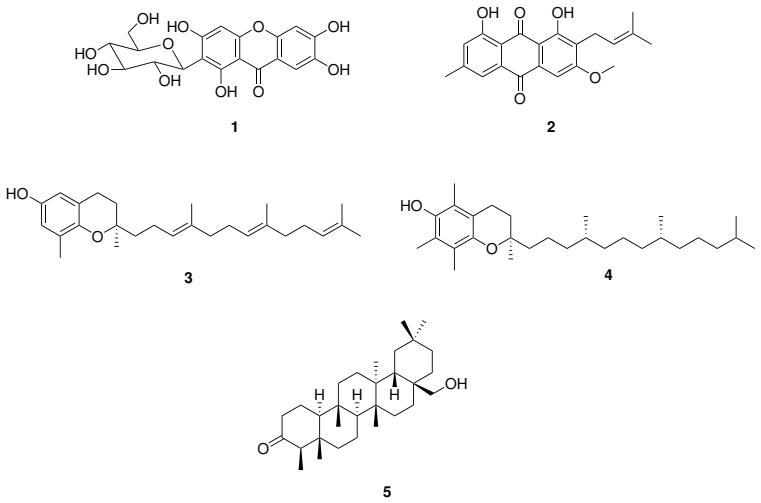

Fig. 1 Phenolic compounds identified as main components in the leave extract of *C. cochinchinense*: (**1**), mangiferin; (**2**), vismiaquinone A; (**3**), δ-tocotrienol; (**4**), α-tocopherol; and (**5**), canophyllol.

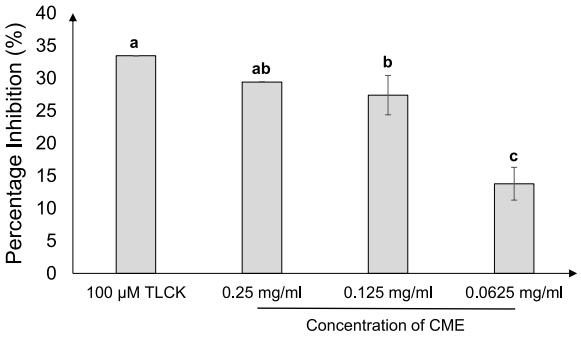

Fig. 2 Inhibition of Kgp activity after treatment with TLCK (positive control) and different concentrations of CME. Data are expressed as means ± SD ($n = 3$). Bars with different alphabets are significantly different from each other, $p < 0.05$.

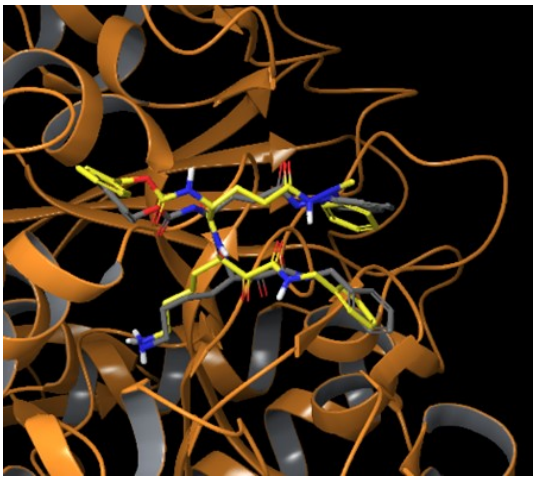

Fig. 3 Superimposition of re-docked KYT-36 (yellow) with co-crystallised KYT-36 (grey) in the binding pocket of Kgp (PDB ID: 6I9A).

Table 1 Docking scores of KYT-36 and the five ligands based on Glide SP protocol.

Compound	Docking score (kcal/mol)
KYT-36	−9.345
Mangiferin	−5.970
Vismiaquinone A	−4.485
δ-Tocotrienol	−4.461
α-Tocopherol	−4.251
Canophyllol	−4.011

Molecular docking of selected ligands against Kgp

The reference ligand (KYT-36, a co-crystallised ligand in 6I9A) was re-docked into the binding pocket of Kgp protein to validate the docking protocols employed. The binding mode of the re-docked ligand was then compared with that of the co-crystallised ligand; both ligands were found closely superimposed onto each other and had similar binding modes within the binding pocket of 6I9A (Fig. 3). The RMSD between the re-docked KYT-36 and the co-crystallised KYT-36 was found to be 1.8429 Å. Considering that 2.0 Å is the threshold value differentiating between correct and incorrect docking solutions as described by Gohlke et al [29], this indicated that the docking protocols used in the present study could well predict the binding pose and the interactions between the ligand and the adjacent residues in the binding site of 6I9A. KYT-36 was found to form a salt bridge and π-cation interaction with Asp516 and Trp513, respectively. It was also engaged in hydrogen bonding with adjacent Thr442,

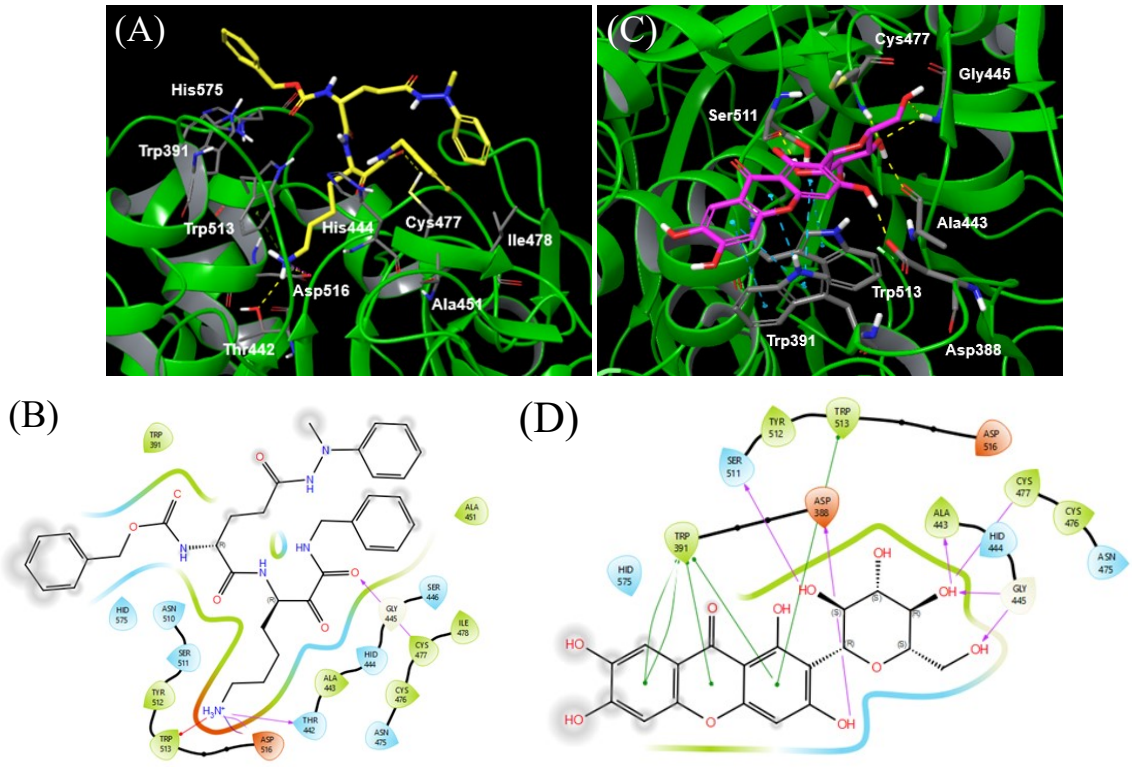

Fig. 4 Binding orientation and interactions of KYT-36 (highlighted in yellow) (A) and mangiferin (highlighted in magenta) (C) in the binding pocket of Kgp (PDB ID: 6I9A). Blue dotted line, π-π stacking; yellow dotted line, hydrogen bonding; green dotted line, π-cation interaction; and magenta dotted line, salt bridge. 2D ligand interaction diagrams of KYT-36 (B) and mangiferin (D) depicting interactions between the ligand and binding site residues. Green line, π-π stacking; purple line, hydrogen bonding; red line, π-cation interaction; and red-blue line, salt bridge.

Cys477, and Asp516. Besides, it was also delineated by residues in proximity, such as Trp391, Ala451, His444, and Ile478 (Fig. 4(A,B)).

All five ligands were found situated within the binding cleft at the cusp. Superimposition of the five ligands in the binding cleft was illustrated in Fig. S2. Among the ligands, mangiferin (**1**) involved in a substantial number of interactions with adjacent residues of the binding pocket, including Asp388, His444, Gly445, Cys477, Trp391, Tyr512, Trp513, and His575. Specifically, magniferin engaged by hydrogen bonding with Asp388, Ala443, Gly445, Cys477, and Ser511; while π-π stacking interaction was observed with Trp391 and Trp513. In addition, the ligand performed interactions with hydrophobic residues, such as Cys476 and Tyr512; and polar residues, like His444 and His575 (Fig. 4(C,D)). On the other hand, vismiaquinone (**2**), δ-tocotrienol (**3**), α-tocopherol (**4**), and canophyllol (**5**) performed same types of binding interactions with residues in vicinity, such as hydrogen bonding, π-π stacking and hydrophobic interaction; but with relatively less numbers of interactions in comparison to mangiferin. The binding orientation and interactions of these four ligands in the binding pocket of Kgp were illustrated in Fig. S3–Fig. S6. The docking scores of KYT-36 and the ligands were tabulated in Table 1.

Kgp enzymatic assay for mangiferin

Based on the molecular docking results, mangiferin was the best inhibitor among the phytocompounds identified in *C. cochinchinense* extracts. In view of that, the inhibitory effects of mangiferin and YLCK (the positive control) were compared. The results revealed that the IC_{50} of mangiferin (134.2 ± 9.36 μM) was not significantly different from the positive control (108.4 ± 20.76 μM).

Identification and quantification of mangiferin in CME

HPLC was used to confirm the presence of mangiferin in CME. The mangiferin showed its identity at retention time of 2.69 min under isocratic system (Fig. 5). With reference to the standard curve (Fig. S1), it was found that the relative contents of mangiferin in *C. cochinchinense* was 55% in 1 mg/ml of extract. Thus,

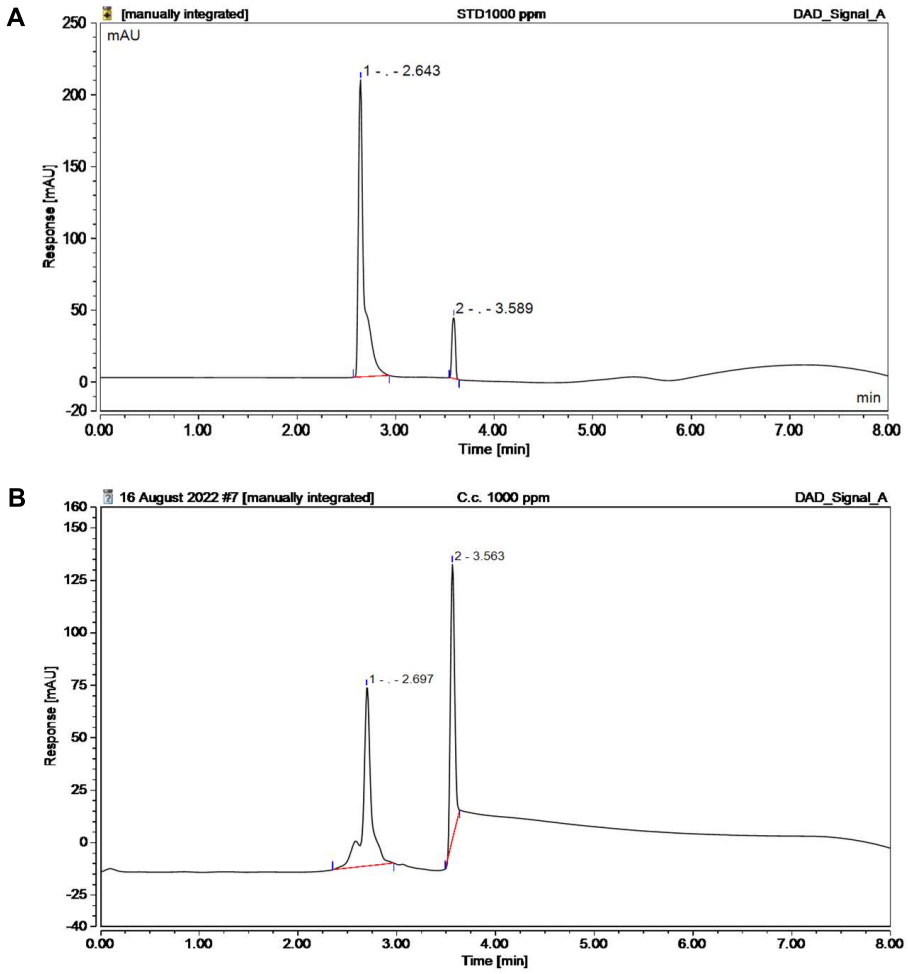

Fig. 5 Chromatograms of xanthone, mangiferin in: (A), standard (⩾ 98%); and (B), CME. Both peaks appearing in the chromatograms are indicative of mangiferin and its isomer.

it was deduced that this bioactive compound might play a significant role in the exertion of Kgp inhibitory effect. Isomerism was also observed in the current study, which was supported by another study reporting the presence of mangiferin isomer in the HPLC profile of coffee leaves [30].

DISCUSSION

The Kgp assay employed to test the inhibitory activities of the plant extracts is mainly based on the enzymatic hydrolysis of the substrate, Ac-Lys-ρNA, with a chromogenic leaving group [24]. During the hydrolysis, the peptide-ρNA bond will be cleaved; and *p*-nitroaniline, that absorbs light at 405 nm, will be released. Inhibition of Kgp activity by plant extracts interfered with the cleavage of the substrate and, thus, resulting in lower absorbance as compared with the untreated control.

As reported previously, a number of polyphenolic-rich plant extracts were shown to be potential Kgp inhibitor such as sword bean [11], roselle calyx [31], green tea [12], tart cherry [32], and fennel [33]. In our present study, we found that the CME could inhibit this bacterial protease as well. Explicitly, the inhibitory effect of CME was comparable to that of roselle calyx [31] but stronger than tart cherry [32]. At different concentrations of 0.0625, 0.125 and 0.250 mg/ml, the CME inhibited Kgp activities by 14%, 27%, and 29% while tart cherry showed inhibition of 8%, 17%, and 38%, respectively. However, both green tea and *n*-hexane extracted fennel were better Kgp inhibitors than CME; as they displayed inhibitory action of more than 50% at a low concentration of 0.06 mg/ml.

C. cochinchinense leaves were reported to mainly contain phenolic components such as mangiferin, vismiaquinone A, α-tocopherol, and δ-tocotrienol; and canophyllol, which is a triterpene [1]. These phytocompounds were used in the molecular docking analysis to evaluate their binding interactions in the active site of Kgp. Based on the docking results, mangiferin (**1**) formed a total of six hydrogen bonds with adjacent

residues. One hydrogen bond was formed between the hydroxyl groups on xanthone nucleus and the carboxylate side chain of Asp388, while another hydroxyl group of C6-glucosyl moiety engaged in forming three hydrogen bonds with –C=O backbone of Ala443 as well as -NH backbone of Gly445 and Cys477. The other two hydrogen bonds were observed between the -NH backbone of Gly445 and –C=O backbone of Ser511 through adjacent methoxy and another hydroxyl group on the glucosyl moiety, respectively. Several π-π stacking interactions were seen between the xanthone nucleus of ligand and indole side chains of Trp391 and Trp513. Hydrophobic residues, Cys476 and Tyr512, bordered the non-polar moieties of ligand as well. Furthermore, polar residues, including His444 and His575, were also found to interact with polar groups of the ligand such as hydroxyl groups on the xanthone nucleus and glucosyl moiety (Fig. 4(C,D)). Among all the residues, Asp388, His444, Gly445, Cys477, Trp391, Tyr512, and Trp513 have been shown to play the important role in ligand binding and recognition [15].

On the contrary, prenyl group on the C2 position of anthraquinone nucleus in vismiaquinone (**2**) failed to form any hydrogen bonding with residues in the binding site as compared with the glucosyl moiety in mangiferin; nonetheless, a hydrogen bonding (via Ser511) and π-π stacking interactions (via Trp391 and Trp513) were observed with the one of the hydroxyl groups and anthraquinone nucleus, respectively (Fig. S3(A,B)). Similarly, the elongated unsaturated isoprenoid side chain and alkyl chain in δ-tocotrienol (**3**) (Fig. S4(A,B)) and α-tocopherol (**4**) (Fig. S5(A,B)) were also unable to engage in any hydrogen bonding with nearby residues. The phenyl group of chromanol ring in δ-tocotrienol (**3**) was found to form a π-π stacking interaction with Trp391, while the hydroxyl on the phenyl group of chromanol ring in α-tocopherol (**4**) formed a hydrogen bonding with Thr574. Likewise, the rigid fused ring structure of canophyllol (**5**) could barely form hydrogen bonding with residues in proximity; a hydroxyl group extended from the structure was found to form a hydrogen bonding with adjacent Trp391 (Fig. S6(A,B)). Indeed, higher negative docking score indicated tighter binding at the target site [34]. The considerable number of hydrogen bonds observed for mangiferin is deduced to have contributed to its higher negative docking score attained in relative to the other compounds (Table 1). Hence, it was suggested that mangiferin is the potential phytochemical that confers the inhibitory activities against Kgp. In comparison to KYT-36, the presence of strong non-covalent interaction of salt-bridge between terminal ε-amino group of KYT-36 with carboxylate side chain of Asp516 and π-cation interaction between the ε-amino group of KYT-36 with phenyl side chain of Trp513 (Fig. 4(A,B)) could have contributed to its higher docking score than that of mangiferin (Table 1). Several hydrogen bonds were also formed between the –C=O carbonyl and terminal ε-amino groups of KYT-36 with Thr442, Cys477, and Asp516. Hydrophobic benzyl and phenyl groups of KYT-36 were found to interact with nearby residues, such as Trp391, Ala451, His444, and Ile478 (Fig. 4(A,B)). These binding interactions and residues were similar with those reported by Guevara et al [15] which described the crystal structure of Kgp co-crystallised with KYT-36.

The results of HPLC analysis further confirmed the presence of mangiferin as a major xanthone in *C. cochinchinense*. Previously, mangiferin was reported to be one of major antioxidant compounds in the leave extract of *C. cochinchinense* [35]. The chromatograms generated from our recent work (Fig. 5) also revealed the existence of mangiferin isomer. Isomangiferin was normally present in lower concentration than mangiferin [30]. Interestingly, the results obtained from this analysis indicated that the abundance of isomangiferin surpassed that of the main compound. Hence, further study should be performed to determine the effects of mangiferin isomers in *C. cochinchinense* towards various bioactivities.

With the molecular docking results substantiating the potential of mangiferin in conferring inhibition towards the Kgp, its activity was therefore compared with the positive control TLCK for the *in vitro* Kgp inhibitory activities. TLCK, also known as N-α-tosyl-L-lysine-chloromethyl-ketone hydrochloride, was selected as the positive control because it is an irreversible cysteine protease inhibitor known to inhibit the Kgp activity. It functions by reacting non-selectively with the thiol group present in the active site of the enzyme, hence inactivating its catalytic activity [36]. Based on the IC_{50} values obtained from mangiferin (134.20 ± 9.36 μM) and TLCK (108.4 ± 20.76 μM), we concluded that the two compounds possessed significantly comparable activities. This experimental finding was congruent with the high docking score observed with mangiferin in the molecular docking studies. However, the synthetic TLCK cannot be used in the prevention and the treatment of periodontitis as it is toxic to oral epithelial cells at the inhibitory concentration for Kgp activity [11].

Comparison of Kgp inhibitory effect of mangiferin with epigallocatechin-3-gallate (EGCG), a pure polyphenolic compound isolated from green tea; it was revealed that mangiferin was a more superior inhibitor. EGCG demonstrated a dose dependent inhibitory activity from 31.25 μM to 250 μM but with lower inhibitory potential ranging from 5% to 15% [12]. In the present study, mangiferin at a low concentration of 12.5 μM was able to inhibit the Kgp by 6.26%. This indicated that the mangiferin exerted a higher degree of inhibition towards this protease in comparison to the EGCG. However,

mangiferin exhibited slightly weaker inhibitory effect compared with the other two polyphenols; Sanggenol A extracted from *Morus alba* root bark [13] and quercetin (3,3′,4′,5,7-pentahydroxyflavone) present in vegetables and fruits [14]. Sanggenol A and quercetin inhibited approximately 10% of Kgp activity at concentrations of 10 μM and 12.5 μM, respectively.

Mangiferin has not only a strong antioxidative nature but also neuroprotective abilities. Its antioxidative nature was the key contributing factor to its neuroprotective potential as it protected the neurons against oxidative stress in AD patients [37]. Mangiferin is a strong ROS scavenger as well as an efficient metal chelator [38]. Furthermore, mangiferin could enhance the endogenous antioxidative system by increasing the enzymatic activities of SOD and catalase [37] like another neuroprotective phytochemical, resveratrol [39].

Moreover, mangiferin was found to mitigate mitochondrial damage by inhibiting the activation of caspase. The caspase cascade was normally initiated by the discharge of cytochrome c from the inner mitochondrial membrane into the cytosol, eventually resulting in the apoptotic process. With the attenuation of cytochrome c by mangiferin in the cytosol, the apoptosis process was reduced; and, thus, both cell death and neuronal injury were prevented [37]. The present research was the first to report on the inhibition of Kgp by mangiferin. With this ability, mangiferin would be able to mitigate the cleavage and the hyperphosphorylation of Tau protein as well as formation of NFTs [2]. Furthermore, the inactivation of NLRP3 inflammasome and neuronal NLRP1 due to Kgp inhibition would block the release of interleukins, IL-1β and IL-18, the causal agents of pyroptosis among neuronal cells. Neuroinflammation by intraneuronal Kgp due to the activation of caspase-1 would certainly be hindered all together. In addition, mangiferin was reported for being able to cross the blood brain barrier to confer neuronal protection. Traces of mangiferin were detected in the brain of rats orally administered with the extract from *Rhizoma anemarrhenae* [40].

CONCLUSION

To date, there has been no effective therapeutic agent that can retard or attenuate AD progression. As Kgp from *P. gingivalis* has been linked to the pathogenesis of AD, our findings certainly highlighted the potential of mangiferin as inhibitor of Kgp for future treatment of AD. Furthermore, in our previous work, we reported the ability of this compound to inhibit PAD, another virulence factor of *P. gingivalis*, that is associated with AD [1]. As such, *in vivo* studies using animal models are vital to further validate the results obtained to confirm mangiferin, a dual inhibitor of both virulence factors of *P. gingivalis*, as a novel treatment strategy for Alzheimer's disease.

Appendix A. Supplementary data

Supplementary data associated with this article can be found at http://dx.doi.org/10.2306/scienceasia1513-1874.2024.073.

Acknowledgements: The authors wish to thank Tunku Abdul Rahman University of Management and Technology (TAR UMT) and International Medical University (IMU) for the financial support through TAR UMT Internal Research Grant Scheme, project number: UC/I/G2020-00062, and IMU Internal Research Grants, project number: MAPC I/2021 (01) and BPC I-2023 (01) as well as the usage of facilities during the progress of this research work.

REFERENCES

1. Tan SA, Yam HC, Cheong SL, Chow YC, Bok CY, Ho JM, Lee PY, Gunasekaran B (2022) Inhibition of *Porphyromonas gingivalis* peptidyl arginine deiminase, a virulence factor, by antioxidant-rich *Cratoxylum cochinchinense*: *in vitro* and *in silico* evaluation. *Saudi J Biol Sci* **29**, 2573–2581.
2. Ryder MI (2020) *Porphyromonas gingivalis* and Alzheimer disease: recent findings and potential therapies. *J Periodontol* **91**, S45–S49.
3. Dominy SS, Lynch C, Ermini F, Benedyk M, Marczyk A, Konradi A, Nguyen M, Haditsch U, et al (2019) *Porphyromonas gingivalis* in Alzheimer's disease brains: evidence for disease causation and treatment with small-molecule inhibitors. *Sci Adv* **5**, eaau3333.
4. Chu J, Lauretti E, Praticò D (2017) Caspase-3-dependent cleavage of Akt modulates tau phosphorylation via GSK3β kinase: implications for Alzheimer's disease. *Mol Psychiatry* **22**, 1002–1008.
5. Sandhu P, Naeem MM, Lu C, Kumarathasan P, Gomes J, Basak A (2017) Ser(422) phosphorylation blocks human tau cleavage by caspase-3: biochemical implications to Alzheimer's disease. *Bioorg Med Chem Lett* **27**, 642–652.
6. Jiang S, Bhaskar K (2020) Degradation and transmission of tau by autophagic-endolysosomal networks and potential therapeutic targets for tauopathy. *Front Mol Neurosci* **13**, 586731.
7. Fleetwood AJ, Lee MKS, Singleton W, Achuthan A, Lee MC, O'Brien-Simpson NM, Cook AD, Murphy AJ, et al (2017) Metabolic remodeling, inflammasome activation, and pyroptosis in macrophages stimulated by *Porphyromonas gingivalis* and its outer membrane vesicles. *Front Cell Infect Microbiol* **7**, 351.
8. Venegas C, Kumar S, Franklin BS, Dierkes T, Brinkschulte R, Tejera D, Vieira-Saecker A, Schwartz S, et al (2017) Microglia-derived ASC specks cross-seed amyloid-β in Alzheimer's disease. *Nature* **552**, 355–361.
9. Saadipour K (2017) TREM1: A potential therapeutic target for Alzheimer's disease. *Neurotox Res* **32**, 14–16.
10. Kim J, Basak JM, Holtzman DM (2009) The role of apolipoprotein E in Alzheimer's disease. *Neuron* **63**, 287–303.
11. Nakatsuka Y, Nagasawa T, Yumoto Y, Nakazawa F, Furuichi Y (2014) Inhibitory effects of sword bean extract on alveolar bone resorption induced in rats by *Porphyromonas gingivalis* infection. *J Periodont Res* **49**, 801–809.
12. Lagha AB, Groeger S, Meyle J, Grenier D (2018) Green tea polyphenols enhance gingival keratinocyte integrity

and protect against invasion by *Porphyromonas gingivalis*. *Pathog Dis* **76**, fty030.
13. King G, Jefferson M, Thomas EL, Stein SH, Jefferia JH, Babu JP (2019) Inhibition of *Porphyromonas gingivalis* gingipain activity by prenylated flavonoid, Sanggenol A. *On J Dent Oral Health* **2**, 000536.
14. He Z, Zhang X, Song Z, Li L, Chang H, Li S, Zhou W (2020) Quercetin inhibits virulence properties of *Porphyromas gingivalis* in periodontal disease. *Sci Rep* **10**, 18313.
15. Guevara T, Rodríguez-Banqueri A, Lasica AM, Ksiazek M, Potempa BA, Potempa J, Gomis-Rüth FX (2019) Structural determinants of inhibition of *Porphyromonas gingivalis* gingipain K by KYT-36, a potent, selective, and bioavailable peptidase inhibitor. *Sci Rep* **9**, 4935.
16. Olsen I, Potempa J (2014) Strategies for the inhibition of gingipains for the potential treatment of periodontitis and associated systemic diseases. *J Oral Microbiol* **6**, 24800.
17. Thu ZM, Aung HT, Sein MM, Maggiolini M, Lappano R, Vidari G (2017) Highly cytotoxic xanthones from *Cratoxylum cochinchinense* collected in Myanmar. *Nat Prod Commun* **12**, 1934578X1701201127.
18. Tang SY, Whiteman M, Jenner A, Peng ZF, Halliwell B (2004) Mechanism of cell death induced by an antioxidant extract of *Cratoxylum cochinchinense* (YCT) in Jurkat T cells: the role of reactive oxygen species and calcium. *Free Rad Biol Med* **36**, 1588–1611.
19. Chailap B, Nuanyai T, Puthong S, Buakeaw A (2017) Chemical constituents of fruits and leaves of *Cratoxylum cochinchinense* and their cytotoxic activities. *Naresuan Uni J Sci Technol* **25**, 22–30.
20. Lv Y, Ming Q, Hao J, Huang Y, Chen H, Wang Q, Yang X, Zhao P (2019) Anti-diabetic activity of canophyllol from *Cratoxylum cochinchinense* (Lour.) Blume in type 2 diabetic mice by activation of AMP-activated kinase and regulation of PPARγ. *Food Funct* **10**, 964–977.
21. Walia V, Chaudhary SK, Kumar Sethiya N (2021) Therapeutic potential of mangiferin in the treatment of various neuropsychiatric and neurodegenerative disorders. *Neurochem Int* **143**, 104939.
22. Du Z, Fanshi F, Lai YH, Chen JR, Hao E, Deng J, Hsiao CD (2019) Mechanism of anti-dementia effects of mangiferin in a senescence accelerated mouse (SAMP8) model. *Biosci Rep* **39**, BSR20190488.
23. Chen F, Wang N, Tian X, Su J, Qin Y, He R, He X (2023) The protective effect of mangiferin on formaldehyde-induced HT22 cell damage and cognitive ompairment. *Pharmaceutics* **15**, 1568.
24. Potempa J, Nguyen KA (2007) Purification and characterization of gingipains. *Curr Protoc Protein Sci* **49**, 21.20.1–21.20.27.
25. Maestro (2021) *Schrödinger*, LLC, New York, NY.
26. LigPrep (2021) *Schrödinger*, LLC, New York, NY.
27. Epik (2021) *Protein Preparation Wizard*, Schrödinger, LLC, New York, NY.
28. Friesner RA, Banks JL, Murphy RB, Halgren TA, Klicic JJ, Mainz DT, Repasky MP, Knoll EH, et al (2004) Glide: a new approach for rapid, accurate docking and scoring. 1. Method and assessment of docking accuracy. *J Med Chem* **47**, 1739–1749.
29. Gohlke H, Hendlich M, Klebe G (2000) Knowledge-based scoring function to predict protein-ligand interactions. *J Mol Biol* **295**, 337–356.
30. Campa C, Mondolot L, Rakotondravao A, Bidel LP, Gargadennec A, Couturon E, La Fisca P, Rakotomalala JJ, et al (2012) A survey of mangiferin and hydroxycinnamic acid ester accumulation in coffee (Coffea) leaves: biological implications and uses. *Ann Bot* **110**, 595–613.
31. Sulistyani H, Fujita M, Nakazawa F (2016) Effect of roselle calyx extract on gingipain activity, production of inflammatory cytokines, and oral bacterial morphology. *J Microbiol Biotech Food Sci* **6**, 961–965.
32. Ben Lagha A, Pellerin G, Vaillancourt K, Grenier D (2021) Effects of a tart cherry (*Prunus cerasus* L.) phenolic extract on *Porphyromonas gingivalis* and its ability to impair the oral epithelial barrier. *PLoS One* **16**, e0246194.
33. Yoshino N, Ikeda T, Nakao R (2022) Dual inhibitory activity of petroselinic acid enriched in fennel against *Porphyromonas gingivalis*. *Front Microbiol* **13**, 816047.
34. Pantsar T, Poso A (2018) Binding affinity via docking: Fact and fiction. *Molecules* **23**, 1899.
35. Tang SY, Whiteman M, Peng ZF, Jenner A, Yong EL, Halliwell B (2004) Characterization of antioxidant and antiglycation properties and isolation of active ingredients from traditional Chinese medicines. *Free Rad Biol Med* **36**, 1575–1587.
36. Griscavage JM, Wilk S, Ignarro LJ (1995) Serine and cysteine proteinase inhibitors prevent nitric oxide production by activated macrophages by interfering with transcription of the inducible NO synthase gene. *Biochem Biophys Res Commun* **215**, 721–729.
37. Alberdi E, Sánchez-Gómez MV, Ruiz A, Cavaliere F, Ortiz-Sanz C, Quintela-López T, Capetillo-Zarate E, Solé]-Domènech S, Matute C (2018) Mangiferin and morin attenuate oxidative stress, mitochondrial dysfunction, and neurocytotoxicity, induced by amyloid beta oligomers. *Oxid Med Cell Longev* **2018**, 2856063.
38. Pardo Andreu G, Delgado R, Velho J, Inada NM, Curti C, Vercesi AE (2005) *Mangifera indica* L. extract (Vimang) inhibits Fe^{2+}-citrate-induced lipoperoxidation in isolated rat liver mitochondria. *Pharmacol Res* **51**, 427–435.
39. Li J, Yuan C, Hu X (2023) Protective effects of resveratrol on nerves in rats with Alzheimer's disease. *ScienceAsia* **49**, 275–281.
40. Li YJ, Sui YJ, Dai YH, Deng YL (2008) LC determination and pharmacokinetics study of mangiferin in rat plasma and tissues. *Chromatographia* **67**, 957–960.

Appendix A. Supplementary data

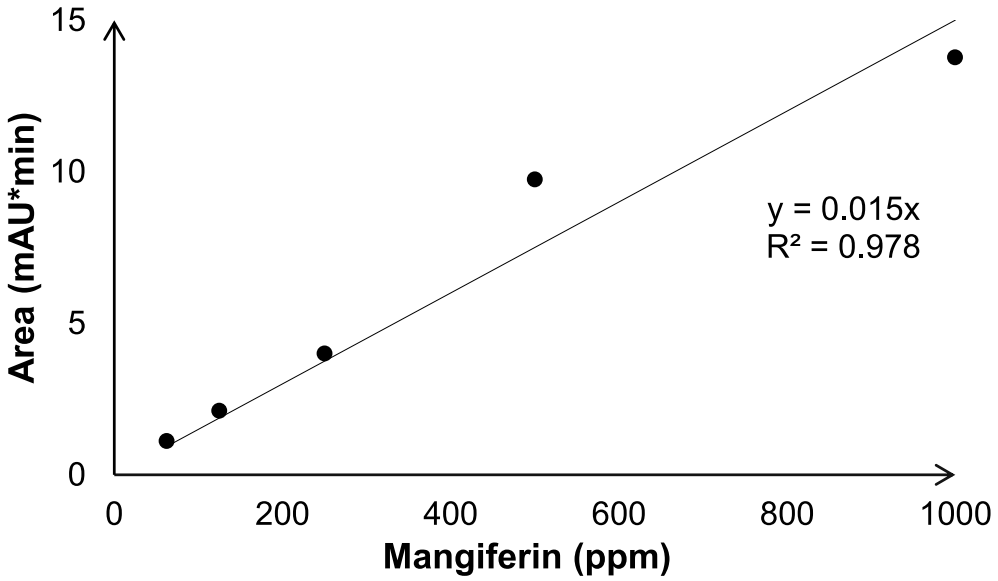

Fig. S1 Mangiferin calibration curve.

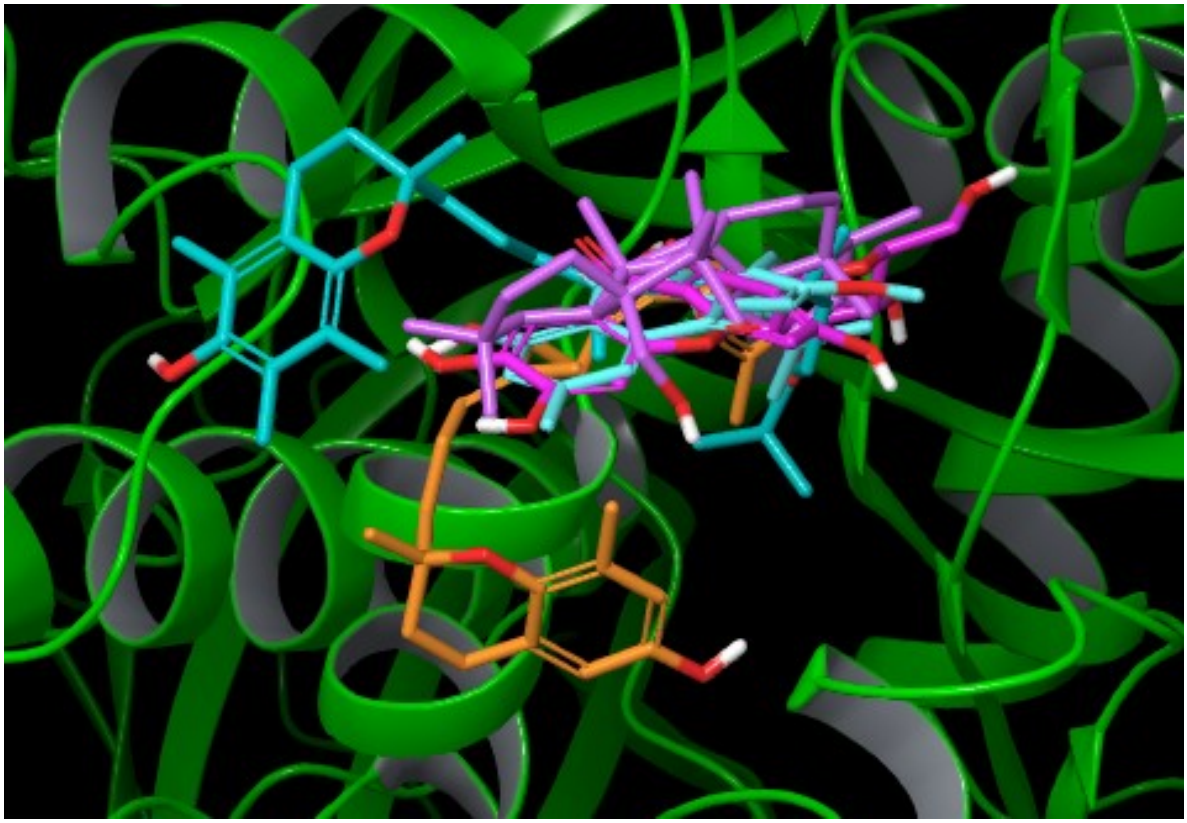

Fig. S2 Superimposition of mangiferin (magenta), vismiaquinone A (cyan), δ-tocotrienol (orange), α-tocopherol (blue), and canophyllol (purple) within the binding cleft of Kgp.

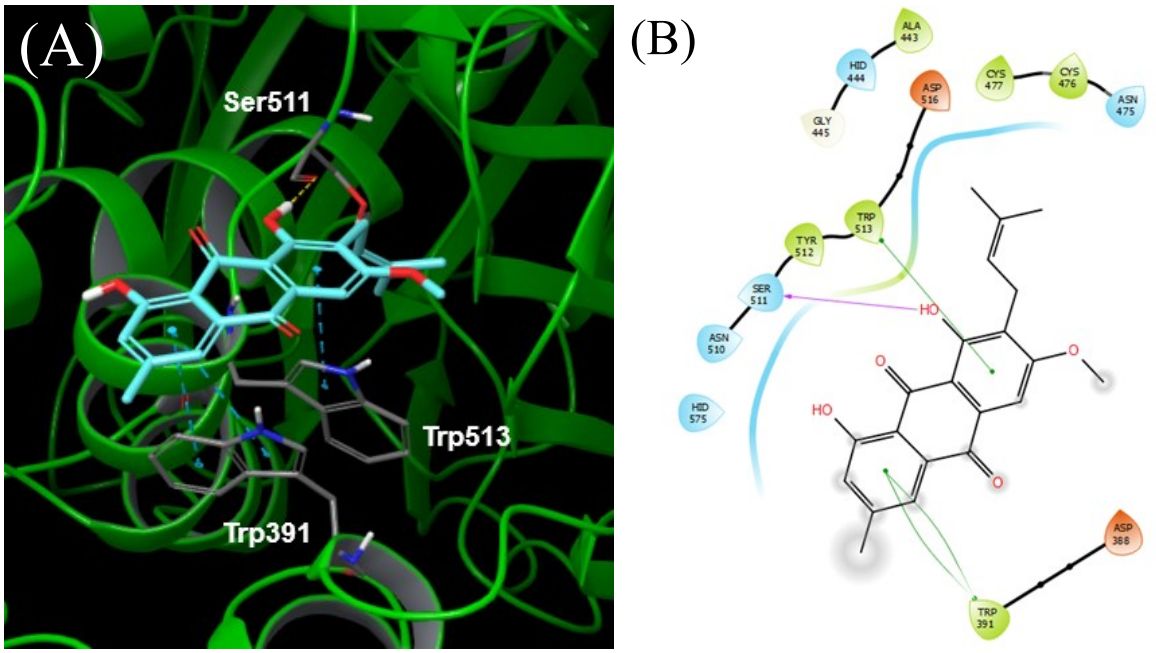

Fig. S3 Binding orientation and interaction of vismiaquinone A (highlighted in cyan) in the binding pocket of Kgp (PDB ID: 6I9A). (A), binding orientation: blue dotted line, π-π stacking; yellow dotted line, hydrogen bonding. (B), 2D ligand interaction diagrams of vismiaquinone A depicting interactions between the ligand and binding site residues: green line, π-π stacking; purple line, hydrogen bonding.

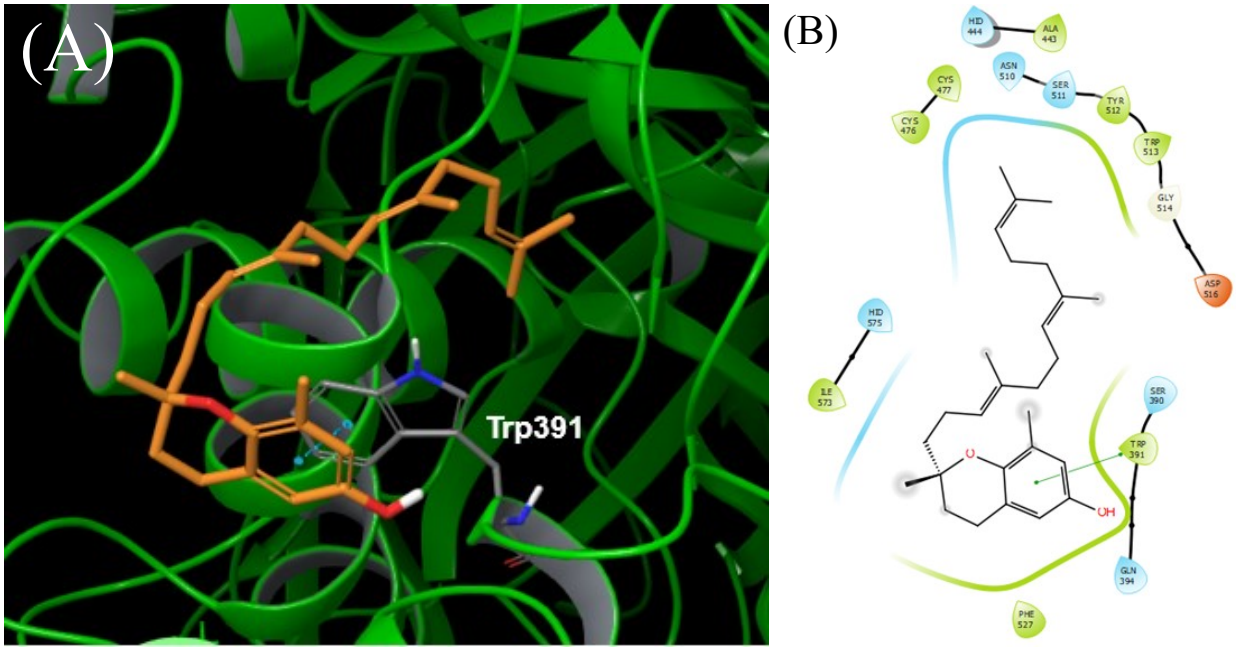

Fig. S4 Binding orientation and interaction of δ-tocotrienol (highlighted in orange) in the binding pocket of Kgp (PDB ID: 6I9A). (A), binding orientation: blue dotted line, π-π stacking; (B), 2D ligand interaction diagrams depicting interactions between the ligand and the binding site residues: green line, π-π stacking.

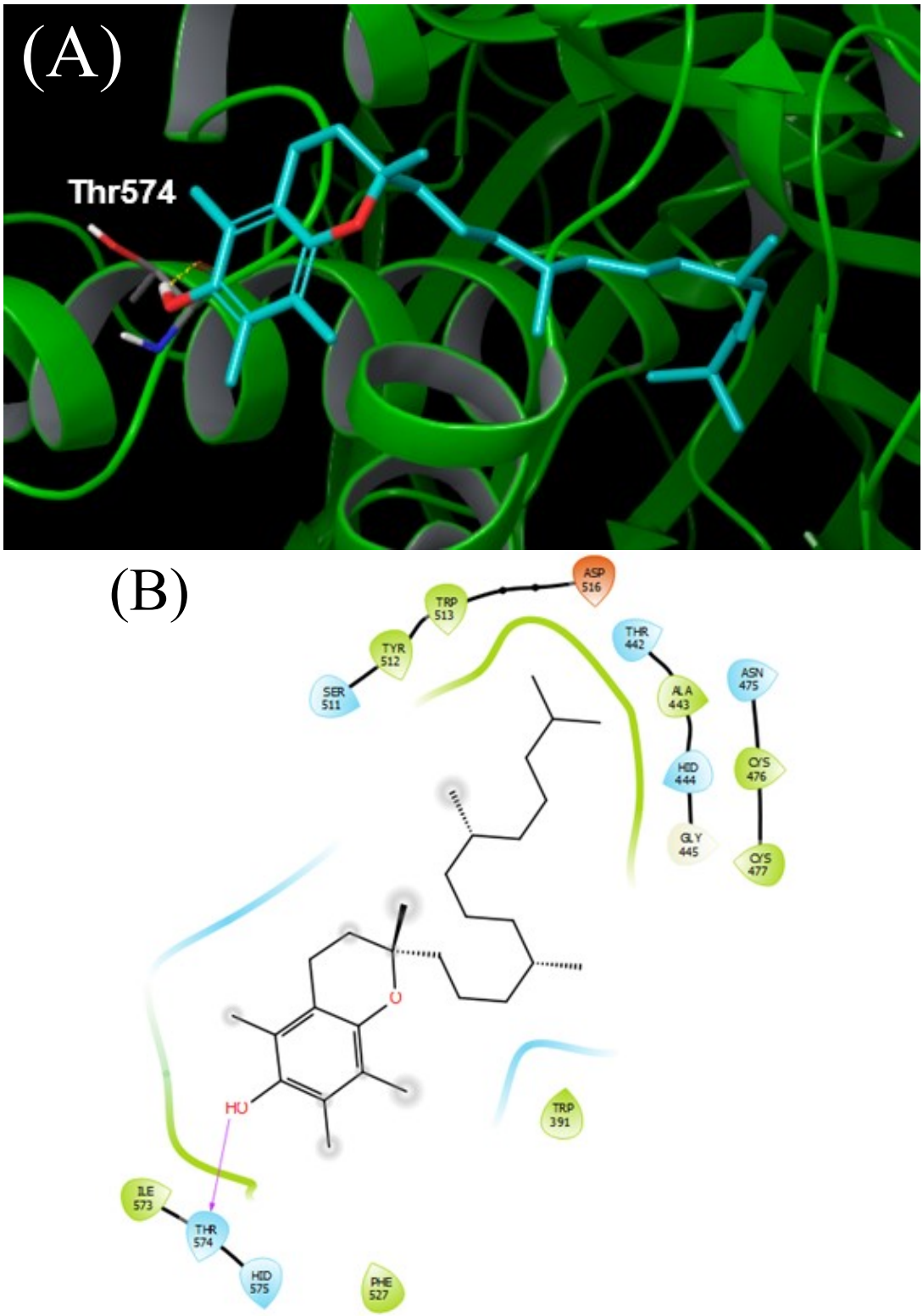

Fig. S5 Binding orientation and interaction of α-tocopherol (highlighted in blue) in the binding pocket of Kgp (PDB ID: 6I9A). (A), binding orientation: yellow dotted line, hydrogen bonding; (B), 2D ligand interaction diagrams depicting interactions between the ligand and binding site residues: purple line, hydrogen bonding.

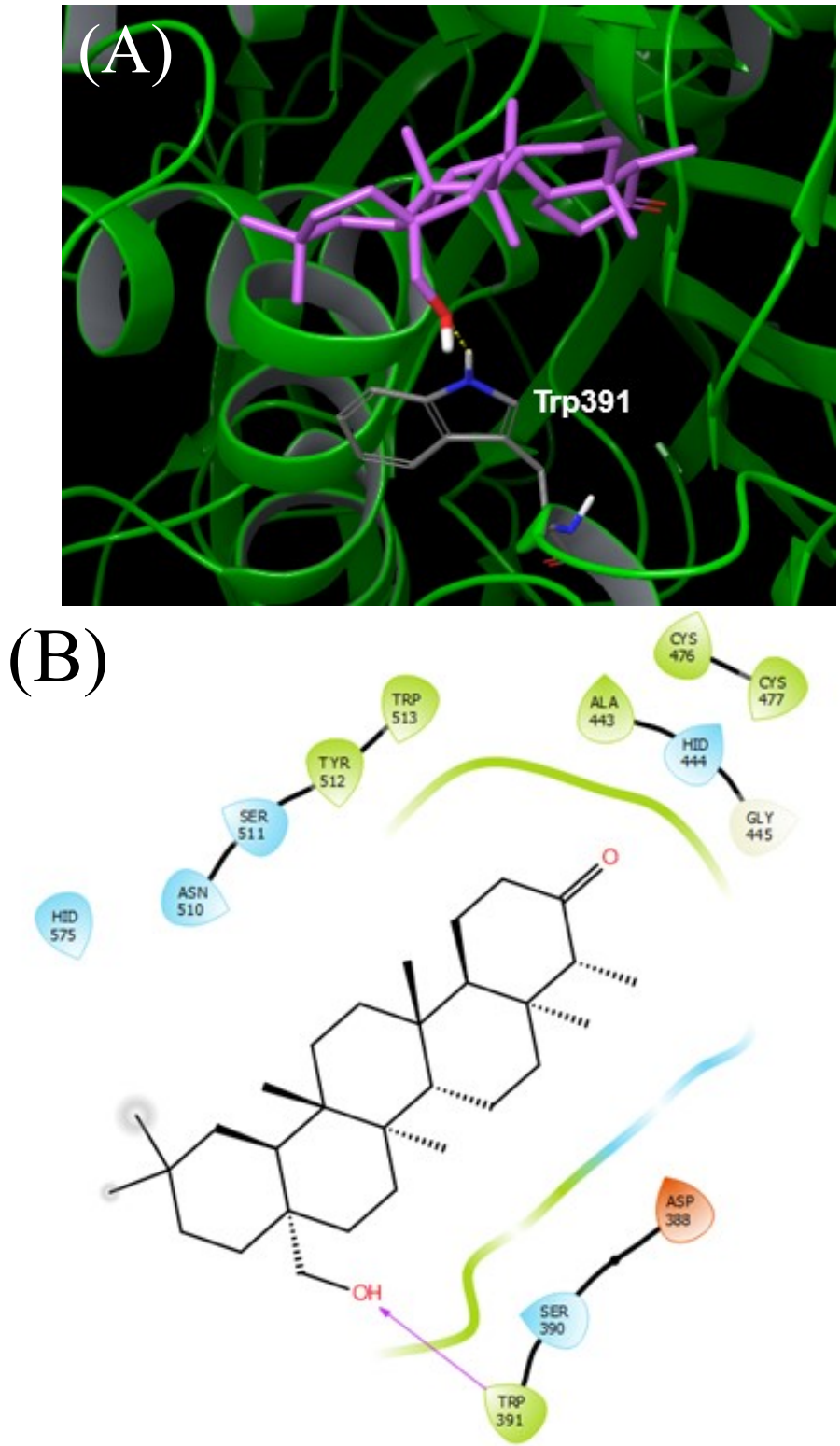

Fig. S6 Binding orientation and interactions of canophyllol (highlighted in purple) in the binding pocket of Kgp (PDB ID: 6I9A). (A), binding orientation: yellow dotted line, hydrogen bonding; (B), 2D ligand interaction diagrams depicting interactions between the ligand and the binding site residues: purple line, hydrogen bonding.